Journal of Power Sources 185 (2008) 549–553

Contents lists available at ScienceDirect

Journal of Power Sources

journal homepage: www.elsevier.com/locate/jpowsour

Short communication

Electrodeposition of cobalt from spent Li-ion battery cathodes by the electrochemistry quartz crystal microbalance technique

E.M. Garcia [a], J.S. Santos [b], E.C. Pereira [b], M.B.J.G. Freitas [a,*]

[a] Universidade Federal do Espírito Santo, Av. Fernando Ferrari 514, Goiabeiras, Vitória, ES, CEP 29075-910, Brazil
[b] Universidade Federal de São Carlos, Rod. Washington Luís (SP-310), Km 235, São Carlos, SP, CEP 13565-905, Brazil

ARTICLE INFO

Article history:
Received 14 May 2008
Received in revised form 5 July 2008
Accepted 7 July 2008
Available online 17 July 2008

Keywords:
Cobalt
Cobalt electrodeposition
Li-ion batteries
Recycling

ABSTRACT

Information about the cobalt electrodeposition mechanism at different pH values was obtained using an electrochemistry quartz crystal microbalance (EQCM) technique as well as potentiodynamic and potentiostatic techniques. Potentiodynamic and potentiostatic electrodeposition of ionic cobalt at pH 5.40 occurs via a direct reduction mechanism. The mass/charge relation was found to be 33.00 g mol^{-1}. At pH 2.70, electrodeposition under potentiodynamic conditions occurs via a mechanism of cobalt reduction with the formation of adsorbed hydrogen. Potentiostatic analysis verified that cobalt reduction occurs simultaneously via direct reduction and with the formation of adsorbed hydrogen. The ratio mass/charge (M/z) is 13.00 g mol^{-1} for potentiodynamic conditions and 26.00 g mol^{-1} for potentiostatic conditions and potentiodynamic conditions. The cobalt electrodissolution occurs directly to Co^{2+} in pH 2.7 and through of the intermediary Co^{+} that is oxidized to Co^{2+} in pH 5.4.

1. Introduction

Li-ion batteries were brought onto the consumer market by Sony Corp. in the early 1990s [1]. Desirable characteristics, such as high energy density, low auto-discharge rate, and high potential difference, made these batteries preferable to the typical Ni–Cd and Ni–MH batteries for many applications. Moreover, Li-ion batteries are less harmful to the environment. For Li-ion batteries, the main materials used are $LiCoO_2$ in the cathode and carbon in the anode [2]. High potentials obtained with these batteries (approximately 3.70 V) hinder the utilization of aqueous electrolytes so that a mixture of lithium organic solvents and inorganic salts is usually required.

Li-ion battery production has been continually increasing since the 1990s, accompanying the consumption growth of portable devices (e.g., cellular phones, microcomputers, and toys). World production of Li-ion batteries increased from 250 to 700 million units between 1998 and 2004 [3]. Residues generated by Li-ion batteries remained at 200–500 tons year^{-1} from 2002 to 2006. Cobalt constitutes between 5 and 20% (m/m) of this residue, while lithium constitutes 2–5% (m/m) of it [3]. The price of cobalt increased from $15 to $54 per kilogram between 2003 and 2004 [4]. Li-ion battery recycling is of great importance for environmental protection; however, economic factors should also be considered. In the USA, Japan, France, Germany, and Sweden, battery recycling is a successful practice. For these regions it is useful to study the established recycling processes of Li-ion batteries [5]. The spent batteries can be recycled by pyrometallurgical or hydrometallurgical processes. The pyrometallurgical process is not desirable due to the emission of toxic gases into the environment. The hydrometallurgical process is thus more favorable from an environment conservation viewpoint. In the hydrometallurgical process, after battery dismantling occurs, the electrodes are dissolved in concentrated acids. After this stage, the resultant solution, which contains metal ions, can be recovered in one of three forms: precipitation, extraction, or electrodeposition. Electrochemical recycling is a viable process to produce cobalt metallic films, alloys, and multilayer deposits with controlled structure and morphology. For this reason, part of cobalt electrochemical recycling is the study of its electrodeposition mechanism. In order to study electrochemical recycling, it is necessary to analyze the mechanism of cobalt electrodeposition at different solution pH.

The production of metallic cobalt is accomplished predominantly via electrodeposition in an aqueous solution [6]. It has been suggested that cobalt electrodeposition at pH < 4.00 occurs together with a hydrogen detachment reaction [6–12]. During this electrodeposition, a rich hydrogen phase can be adsorbed in the deposits, as represented by Eqs. (1)–(4):

$$Co_{(aq)}{}^{2+} + 2e^{-} \rightarrow Co_{(s)}; \quad (1)$$

$$H_{(aq)}{}^{+} + Co_{(s)} + e^{-} \rightarrow CoH_{(ads)}; \quad (2)$$

* Corresponding author. Tel.: +55 27 33352486; fax: +55 27 33352460.
E-mail address: marcosbj@hotmail.com (M.B.J.G. Freitas).

0378-7753/$ – see front matter © 2008 Elsevier B.V. All rights reserved.
doi:10.1016/j.jpowsour.2008.07.011

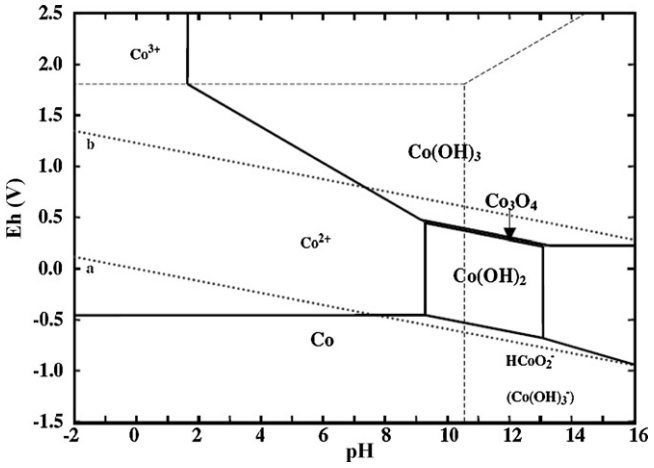

Fig. 1. Pourbaix diagram for Cobalt–H_2O system.

$$H_{(aq)}^{+} + CoH_{(ads)} + e^{-} \rightarrow Co_{(s)} + H_{2(ads)}; \quad (3)$$

$$\text{Total equation}: Co_{(aq)}^{2+} + 2H^{+} + 4e^{-} \rightarrow Co_{(s)} + H_{2(ads)}. \quad (4)$$

At pH > 4.00, the electrodeposition of cobalt occurs via $Co(OH)_2$ forming in the interface electrode solution (chemical stage). In the cobalt electrodeposition process the interface electrode solution becomes alkaline due to the water reduction (Eq. (5)). The local alkalization that occurs in the interface electrode solution can provoke the precipitation of the $Co(OH)_2$ as showed in Pourbaix diagram (Fig. 1). The presence of cobalt hydroxide was confirmed with an electrochemistry quartz crystal microbalance (EQCM) technique, as done by Matsushima et al. [11].

H_3BO_3 was added to the cobalt electrodeposition solution to avoid pH variations in the interface electrode solution. In this case, the electrodeposition of cobalt occurs directly, owing to Eq. (1) [12]. Eqs. (5)–(8) describe the electrodeposition process through formation of a cobalt hydroxide intermediate:

$$2H_2O + 2e^{-} \rightarrow 2OH_{(aq)}^{-} + H_{2(g)}; \quad (5)$$

$$Co_{(aq)}^{2+} + 2OH_{(aq)}^{-} \rightarrow Co(OH)_{2(s)}; \quad (6)$$

$$Co(OH)_{2(s)} + 2e^{-} \rightarrow Co_{(s)} + 2OH_{(aq)}^{-}; \quad (7)$$

$$\text{Total equation}: Co_{(aq)}^{2+} + 2H_2O + 4e^{-} \rightarrow Co_{(s)} + 2OH^{-} + H_{2(g)}. \quad (8)$$

The EQCM technique supplies detailed information about variations in electrodeposition and electrodissolution mass for fine films, as caused by oxidation and reduction processes [13–20]. According to Sauerbrey's equation, frequency variation (Δf) of the quartz crystal can be correlated with the mass variation (Δm) and can be written according to Eq. (9):

$$\Delta f = \left(\frac{-2f_0^2 \Delta m}{A\sqrt{\mu_i \rho_i}}\right) = -\Delta m K \quad (9)$$

where f_0 is the resonance frequency of the quartz crystal, A is the piezoelectric active area, μ_i is the quartz shear modulus, K is the experimental mass coefficient, and ρ_i is the density of quartz.

The current work is a continuation of previous work that studied the electrochemical recycling of cobalt from the spent cathodes of Li-ion batteries [8]. In this work, a greater efficiency for cobalt electrodeposition was found at a potential equal to −1.00 V at all pH values tested (1.50, 2.70, and 5.40). It was observed that the charge efficiency of cobalt electrodeposition decreased with a decrease in the pH of the solution. The cobalt nucleation process was investigated with the help of mathematical models proposed by Scharifker and Hills [21]. In the present work, the electrodeposition mechanism of cobalt thin films has been studied. For this reason the electrochemical quartz crystal microbalance technique was used together with potentiodynamic and potentiostatic techniques to obtain information about the electrodeposition mechanism for cobalt from the cathodes of spent Li-ion batteries. This technique is very effective in the study of the mechanism of metal electrodeposition for thin films. However, deviations from the Sauerbrey's equation occur for thick films. The study of the electrodeposition mechanism is key in electrochemical recycling because it correlates with the structure, morphology, and properties of the cobalt film. The current work aims to clarify the cobalt electrodeposition mechanism as a function of pH. It follows then that the study of the cobalt electrodeposition process is of paramount importance in the electrochemical recycling of cobalt.

2. Experimental

2.1. Electrodeposition solution preparation

Li-ion batteries were manually dismantled and physically separated into their different parts, including the anode, cathode, steel, separators, and current collectors. Electrodes were dried at 80 °C for 24 h and then washed in distilled water at 40 °C for 1 h under agitation to eliminate organic solvents, propylene carbonate (PC), and ethylene carbonate (EC). This procedure also facilitates the detachment of active material from the respective current collectors. Active material was filtered, washed with distilled water at 40 °C to remove potential lithium salts (e.g., $LiPF_6$ and $LiCl_4$) and Cu (from anode current collector), and then dried in air for 24 h. A total of 9.17 g of positive electrode material was dissolved in a solution containing 470.00 ml of HCl 3.00 mol l^{-1} and 30.00 ml of H_2O_2 (30%, v/v). This system was maintained under constant magnetic agitation at 80 °C for 2 h. Cathode dissolution efficiency increases with increasing acid concentration and temperature. The addition of H_2O_2 was necessary to increase cathode dissolution efficiency [22]. H_2O_2 reduces cobalt from a +III oxidation state, which is insoluble in aqueous systems, to a +II oxidation state, which is soluble in aqueous systems. For an active material consisting of $LiCoO_2$, the cathode dissolution reaction is represented by Eq. (10):

$$LiCoO_{2(s)} + 1/2H_2O_{2(l)} + 3HCl_{(aq)} \rightarrow CoCl_{2(aq)} + 1/2O_{2(g)} + LiCl_{(aq)} + 2H_2O_{(l)} \quad (10)$$

The cathode composition was found to be $LiCoO_2$, Co_3O_4, Al, and carbon [8]. The cathode can be contaminated with electrolyte or anode material. Therefore, the leaching solutions used were characterized by atomic absorption spectroscopy (AAS) to detect the presence of lithium, copper, and cobalt. The cobalt and lithium concentrations were both equal to 0.10 mol l^{-1}. The ionic copper concentration was not detected. The ionic lithium does not influence the cobalt electrodeposition because its reduction occurs at a more cathodic potential (−3.02 V). Solutions were buffered using H_3BO_3 at 0.10 mol l^{-1} to maintain the electrodeposition bath pH.

2.2. Electrochemistry quartz crystal microbalance measurements

For ECQM Experiments, a 50.0 ml Pyrex® cell was used. The cover was made of Teflon® and included holes for the introduction of saturated Ag/AgCl/NaCl reference and platinum auxiliary electrodes, with a geometric area of 0.50 cm^2. The working electrode was introduced at the bottom of the cell. Working electrodes were composed of quartz crystal covered with platinum of

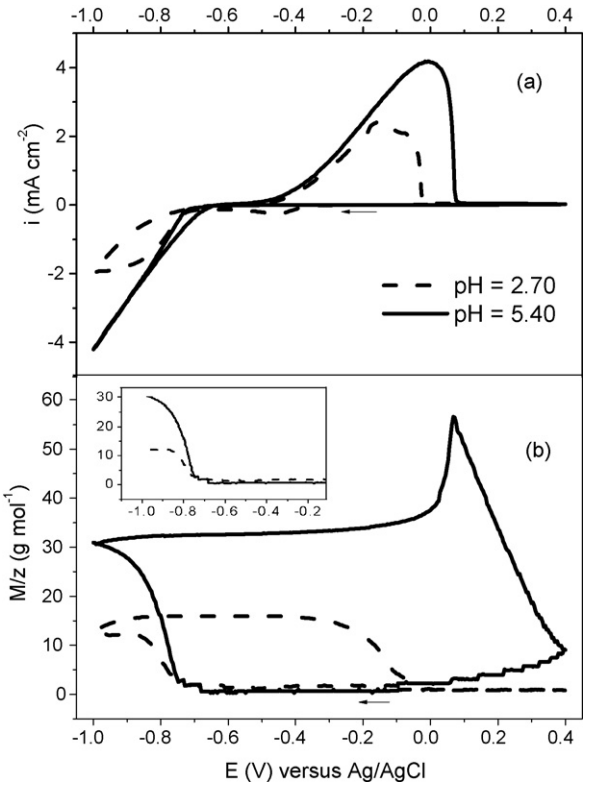

Fig. 2. (a) Cyclic voltammograms curves, cobalt concentration of 0.10 mol l^{-1}, pH 5.40 and 2.7, H_3BO_3 0.10 mol l^{-1} as buffer. The potential scan rate was 20.00 mV s^{-1}. (b) Variation of *M*/*z* as a function of potential.

fundamental frequency of 9.00 MHz (SEIKO) and had a geometric area of 0.20 cm^2. The platinum electrode was cleaned with sulphonitric solution and washed with dilutes. Afterward, it was submitted to an electrochemistry cleaner, which consisted of successive platinum oxidation and reduction cycles in a solution of H_2SO_4 0.10 mol l^{-1} until characteristic cyclic voltammograms curves of the platinum in acid were obtained.

EQCM measurements were accomplished simultaneously with potentiodynamic and potentiostatic studies. For potentiodynamic measurements, the initial potential was 0.00 V, where no reaction occurs at the electrode, and the final potential was −1.00 V. A scan rate of 20.00 mV s^{-1} was used. Potentiostatic measurements were made by applying a potential jump from −0.10 V (no reaction at the electrode) to −0.90 or −1.00 V. The system was polarized for 30 s at these potentials.

EQCM measures were performed using a Quartz Crystal SEIKO EG&G model QCA917 microbalance. This was coupled to a PAR model 263A power supply. The system was managed using M270 software from EG&G EVEN. The frequency measures conversion in mass variation was made with base in Sauerbrey's equation (Eq. (9)). A sensibility coefficient of 858.80 μg Hz^{-1} was used.

3. Results and discussion

3.1. Potentiodynamic and electrochemistry quartz crystal microbalance measurements

Measurements of the potentiodynamic electrodeposition of cobalt coupled to the EQCM technique are shown in Fig. 2. The voltammograms curves for two different pH solutions (2.70 and 5.40) with a scan rate of 20 mV s^{-1} appear in Fig. 2a. Correspondent mass variations on the working electrode are represented in the inset of Fig. 2b. Upon analysis of the voltammogram curve for a pH 2.70 solution (Fig. 2a), during the scan through negative potentials, no processes were observed until a potential of −0.34 V was reached. From this potential, an increase in current density was observed, reaching a maximum value of −0.46 V. As shown in the inset of Fig. 2b, however, no mass variation was observed until a potential of −0.75 V was achieved. From this potential, the current density increased quickly prior to reaching the inversion potential (−1.00 V), which was followed by a mass increase on the platinum electrode. The voltammogram curve obtained for cobalt electrodeposition in a pH 5.40 solution presents similar behavior; however, during the cathodic scan, the current density begins to increase at −0.70 V. At this potential, cobalt deposition onto the platinum electrode was initiated, as shown in the mass variation profile of platinum (inset of Fig. 2b). Current density increased continually until −1.00 V, due to the proton discharge reaction that occurs simultaneously with metallic cobalt deposition.

To study the cobalt electrodeposition mechanism, a curve of mass/charge (*M*/*z*) as a function of the potential was constructed for the both solutions (Fig. 2b). Experimental *M*/*z* values were compared with theoretical values obtained for mechanisms of more probable reactions, such as: (i) the direct electrodeposition reaction of cobalt (Eq. (1)), (ii) the deposition reaction of metallic cobalt with adsorbed hydrogen (Eq. (4)), and (iii) the reduction of cobalt from $Co(OH)_2$ (Eq. (8)). The theoretical *M*/*z* values for reactions (i) through (iii) were, respectively, 29.50 g mol^{-1} ($M_{Co}{}^{2+}/2e^-$; Eq. (1)), 15.25 g mol^{-1} ($M_{Co}{}^{2+} + 2H^+/4e^-$; Eq. (4)), and 14.80 g mol^{-1} ($M_{Co}{}^{2+}/4e^-$; Eq. (8)).

Its value of the *M*/*z* when the cobalt is being deposited with 100% efficiency, i.e., without any other parallel process on the surface of the electrode. If electrochemical processes occur with parallel chemical processes as for example with deposit of mass by precipitation, the ratio *M*/*z* will be higher value than theoretical. If electrochemical process occur with lower or no mass change, the experimental *M*/*z* will be lower than the theoretical value for the reaction considered.

From Fig. 2b, it was observed that experimental *M*/*z* values obtained during cobalt electrodeposition in a solution of pH 5.40 moved toward a value of 32.00 g mol^{-1} as the deposition advanced in the cathodic direction. This result suggests that deposition is occurring in agreement with Eq. (1). Already at pH 2.70, *M*/*z* values tended toward a value of 13.00 g mol^{-1}.

This result suggests that cobalt electrodeposition might be occurring via the formation reaction of $Co(OH)_2$ or by the mechanism of adsorbed hydrogen. As observed by Matsushima et al. [11], however, the formation of $Co(OH)_2$ does not occur in solutions of pH < 2.70. Therefore, the decrease in observed *M*/*z* values might be associated with the formation of adsorbed hydrogen. This reaction occurred in solutions with pH < 2.70 when H_3BO_3 was added as a buffer to prevent local pH variations in the solution. Experimental *M*/*z* values were lower than theoretical values owing to the hydrogen reduction reaction, which decreases the efficiency for cobalt electrodeposition.

The voltammograms curves for cobalt electrodissolution at both analyzed pH values are shown in Fig. 2a. According to Soto et al. [23], peak I can be associated with cobalt oxidation containing hydrogen-rich phase. The shoulder of current II can be related with cobalt electrodissolution without adsorbed hydrogen.

Turning to the anodic scan, cobalt deposition continues until reached the potential of −0.1 V, when is observed a current peak due to the cobalt electrodissolution (Fig. 2a). In Fig. 2b is observed that the ratio *M*/*z* increase to 60.00 g mol^{-1}. That resulted indicate that the metallic Co electrodissolution occurs through a formation of an intermediary Co^{1+} in the interface metal solution. In the following stage, the Co^+ is oxidized to Co^{2+}, as can be see in Eq. (11). Finally,

at potential more positive than 0.100 V, the metallic cobalt film is dissolved and the ratio M/z attains the starting value. This behavior also was observed by Martin et al. [24].

$$Co_{(s)} \rightarrow Co_{(aq)}{}^{+} + H_2O \rightarrow Co_{(aq)}{}^{+2} + OH_{(aq)}{}^{-} + 0.5H_2 \quad (11)$$

3.2. Potentiostatic and electrochemistry quartz crystal microbalance measurements

Chronoamperogram plots and the corresponding variations of M/z as functions of time are shown in Fig. 3. In this case, the potentiostatic electrodeposition of cobalt in a pH 5.40 solution, with −0.90 V applied potential, presented a similar behavior in comparison with potentiodynamic electrodeposition. M/z values for deposition in this pH 5.40 solution tended towards a value of 33.00 g mol^{-1}, which corresponds to the cobalt direct electrodeposition mechanism (Eq. (1)). For electrodeposition in a pH 2.70 solution, M/z values were already near 10.00 g mol^{-1} at the initial deposition stage. The M/z relation continued increasing as the deposition advanced, reaching 22.00 g mol^{-1} by the end of the electrodeposition. The M/z value for cobalt reduction at pH 2.70 was intermediary between direct reduction (M/z = 29.50 g mol^{-1}) and reduction together with adsorbed hydrogen formation (15.25 g mol^{-1}). This result demonstrates that, in some electrode regions, the direct reduction reaction occurs and that, in others, the cobalt reduction reaction, with adsorbed hydrogen formation, occurs.

Behavior similar to that shown in Fig. 3 was also observed for potentiostatic electrodeposition (−1.00 V), which is presented in Fig. 4. In this case, M/z values remained near 33.00 g mol^{-1} throughout electrodeposition in a pH 5.40 solution. For the pH 2.70 solution, M/z values began at approximately 12.00 g mol^{-1} and continued increasing up to a value of 26.00 g mol^{-1} at the end of the process. This M/z can be explained using simultaneous mechanisms, including the direct reduction reaction and the cobalt reduction reaction, with adsorbed hydrogen formation. Comparison of M/z values during potentiostatic electrodeposition at two different potentials (pH 2.70) revealed that M/z was larger when the deposition was performed at a more negative potential. Thus, the potential displacement for more cathodic values increased the cobalt reaction contribution via a mechanism of direct reduction (Eq. (1)).

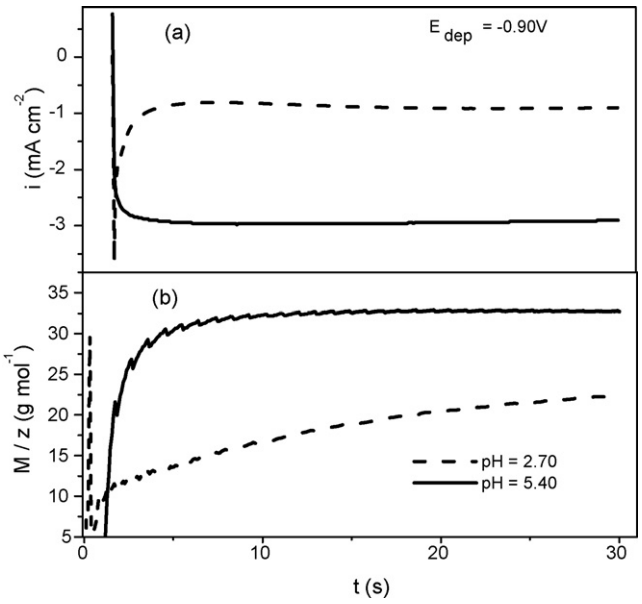

Fig. 3. (a) Chronoamperogram plots, potential applied of −0.90 V, polarized for 30 s at this potential, cobalt concentration of 0.10 mol l^{-1}, pH 5.40 and 2.7, H_3BO_3 0.10 mol l^{-1} as buffer. (b) Variation of M/z as a function of time.

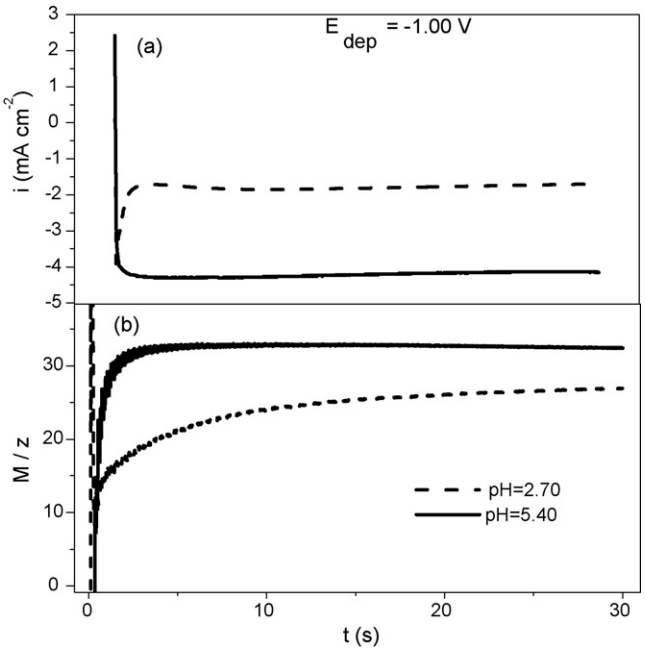

Fig. 4. (a) Chronoamperogram plots, potential applied of −1.00 V, polarized for 30 s at this potential, cobalt concentration of 0.10 mol l^{-1}, pH 5.40 and 2.7, H_3BO_3 0.10 mol l^{-1} as buffer. (b) Variation of M/z as a function of time.

Results obtained for potentiostatic electrodepositions suggest that, at pH 5.40, cobalt reduction occurs by a direct reduction mechanism. For cobalt electrodeposition at pH 2.70 and in the presence of the hydrogen detachment reaction, a simultaneous mechanism of direct reduction and cobalt reduction occurs.

4. Conclusions

Using an EQCM, verified the mechanism for cobalt electrodeposition and correlated it with solution pH and electrochemical conditions. The electrodeposition mechanism occurs via the direct reduction of cobalt (Eq. (1)) for a pH of 5.40 and under potentiodynamic or potentiostatic conditions. The relation value M/z for cobalt electrodeposition at pH 5.40 under potentiodynamic and potentiostatic conditions was equal to 32.00 and 33.00 g mol^{-1}, respectively.

Potentiodynamic electrodeposition of cobalt at pH 2.70 occurs via the mechanism of adsorbed hydrogen, and M/z values tend towards 13.00 g mol^{-1}. The experimental M/z relation was lower than that predicted by theory due to the hydrogen reduction reaction, which decreases the cobalt electrodeposition efficiency. Cobalt potentiostatic electrodeposition at pH 2.70 occurs via simultaneous mechanisms of direct reduction and cobalt reduction in the presence of adsorbed hydrogen. The M/z value was larger for depositions accomplished at a more negative potential. This demonstrates that a more cathodic potential increases the direct cobalt reaction (Eq. (1)) contribution to the simultaneous mechanism of direct reduction.

The cobalt electrodissolution occurs directly to Co^{2+} in pH 2.7 and through of the intermediary Co^{+} that is oxidized to Co^{2+} in pH 5.4.

Acknowledgements

The authors acknowledge MCT-CNPq-FAPES and PETROBRAS for financial support.

References

[1] R. Moshtev, B. Johnson, Journal of Power Sources 91 (2000) 86.
[2] M. Noel, V. Suryanarayanan, Journal of Power Sources 111 (2002) 193.
[3] S.K. Jeong, I. Minoru, I. Yasutoshi, A. Takeshi, O. Zempachi, Journal of Power Sources 175 (2008) 540.
[4] J. Jandova, H. VU, P. Dvorak, Hydrometallurgy 77 (2005) 67.
[5] M.A. Bernardes, R.C.D. Espinosa, S.J.A. Tenorio, Journal of Power Sources 130 (2004) 291.
[6] M.I. Jeffrey, W.L. Choo, P.L. Breuer, Minerals Engineering 13 (2000) 1231.
[7] C. Lupi, M. Pasquali, A.D. Era, Waste Management 25 (2005) 215.
[8] M.B.J.G. Freitas, E.M. Garcia, Journal of Power Sources 171 (2007) 953.
[9] D.R. Gabe, Journal of Applied Electrochemistry 27 (1997) 908.
[10] N. Pradhan, T. Subbaiah, S.C. Das, Journal of Applied Electrochemistry 27 (1997) 713.
[11] T. Matsushima, F.T. Strixino, E.C. Pereira, Electrochimica Acta 51 (2006) 1960.
[12] J.S. Santos, R. Matos, F.T. Strixino, E.C. Pereira, Electrochimica Acta 53 (2007) 644.
[13] A. Krause, M. Uhlemann, A. Gebert, L. Schultz, Electrochimica Acta 49 (2004) 4127.
[14] K.Z. Rozman, A. Krause, K. Leistner, S. Fähler, L. Schultz, H. Schlörb, Journal of Magnetism and Magnetic Materials 314 (2007) 116.
[15] A. Bott, Current Separations 3 (1999) 79.
[16] M.R. Deakin, D.A. Buttry, Analytical Chemistry 61 (1989) 1147.
[17] M. Kemell, H. Saloniemi, M. Ritala, M. Leskela, Electrochimica Acta 45 (2000) 3737.
[18] H.A.K.M. Saloniemi, M. Ritala, M. Leskela, Journal Electroanalytical Chemistry 482 (2000) 139.
[19] M.D. Ward, I. Rubinstein (Eds.), Physical Electrochemistry Principles, Methods, and Applications, Marcel Decker Inc, New York, 1995, p. 293.
[20] S. Jaya, P. Rao, T.G. Prao, Electrochimica Acta 32 (1987) 1073.
[21] B. Scharifker, G. Hills, Journal of Electrochimica Acta 28 (1983) 879.
[22] B. Swain, J. Jeong, J. Lee, G.H. Lee, J.S. Sohn, Journal of Power Sources 167 (2007) 536.
[23] A.B. Soto, E.M. Arce, M.P. Pardavé, I. Gonzalez, Electrochimica Acta 16 (1996) 2647.
[24] A.J. Martin, A.M. Chaparro, L. Daza, Journal of Power Sources 169 (2007) 65.